Line shapes of narrow optical bands: Infrared absorption by *U* centers and heavier impurities in alkali halides

Miguel Lagos*
Facultad de Ingeniería, Universidad de Talca, Campus Los Niches, Curicó, Chile

Felipe Asenjo, Roberto Hauyón, and Denisse Pastén
Departamento de Física, Facultad de Ciencias, Universidad de Chile, Casilla 653, Santiago, Chile

Hernán González, Ricardo Henríquez, and Roberto Troncoso
Departamento de Física, Facultad de Ciencias Físicas y Matemáticas, Universidad de Chile, Casilla 487-3, Santiago, Chile
(Received 18 January 2008; published 27 March 2008)

The shape of the bands for photon absorption and emission by the local constituents of a solid is governed mainly by processes involving many low-energy acoustic phonons. This applies not only to wide bands, such as those exhibited by *F* centers, but also to narrow ones, as those observed for infrared absorption by local vibration modes of *U* centers and heavier impurities. The line shapes are theoretically studied on a general basis to show they provide a nice example to illustrate the power of field theory and methods to reproduce experimental facts. To this aim, the phonon induced broadenings of infrared absorption lines by *U* centers in KCl and KBr, and by substitutional Ag^+ in KI, were calculated to compare theoretical predictions with experiment. The agreement obtained between both is remarkable.

DOI: 10.1103/PhysRevB.77.104305 PACS number(s): 78.20.Bh, 78.30.−j, 78.55.Fv, 71.55.−i

I. INTRODUCTION

The study of the line shapes of light absorption and emission bands by localized centers in solids is a beautiful subject because can be precisely measured, and either are amenable to analytical calculation by the methods of the theory of fields. Historically, however, most of the effort has been done on the optical bands of *F* centers in alkali halides, which are particularly wide, of about 0.2–0.5 eV full width at half height, and rather old means have been employed to analyze the data. Consisting of a single electron trapped by an anionic vacancy in an ionic crystal, without a positive ion core, *F* electrons have a spread wave function, which couples strongly with the neighboring lattice ions. Transitions between *F* electron states cause severe local distortions. Though the method conceived principally by Huang and Rhys[1,2] on the basis of the semiclassical Franck-Condon principle[3,4] to derive the line-shape function has plenty of physical insight, it cannot compete with more recent second-quantized techniques. Although both approaches to the problem yield similar expressions for the main component of the line-shape function, the latter is simpler and fully analytical, gives precise knowledge of the terms that are left aside and how to reincorporate them, and provides reliable information on the range in which the results remain valid. Conversely, the semiclassical basis of the Huang-Rhys theory leaves these aspects uncertain. Perhaps for this reason the theory has been applied to almost only *F* centers, whose wide bands seem more consistent with the Franck-Condon model for the optical transitions in solids.

According to Franck[3] and Condon,[4] electronic transitions occur with no change in the nuclear configuration. The Franck-Condon model relies on a semiclassical picture of the lattice dynamics that follows an internal electronic transition in a point defect, originated by the absorption or emission of a photon. As the interaction of an ion with its neighbors should depend on its excitation state, the process causes a sudden variation of the local lattice forces. Then, the original lattice ceases to be the equilibrium configuration, and the crystal begins to evolve to the distorted structure that balances the new forces. As the electronic excitation is abrupt, the massive crystal ions have not enough time to change their individual dynamical states, and simply commence to oscillate around the new equilibrium sites, starting from the positions, and with the velocities, they had when the transition took place. These positions and velocities correspond to different energies in the distorted and undistorted lattices. Hence, in summary, electronic changes occurring in a crystal constituent involves both a lattice distortion and a transition to a new vibrational state.

This traditional model is expected to work better for systems displaying wide optical bands, because they are associated by the uncertainty principle to transitions involving shorter times, and hence satisfy better the assumption of a sudden change in the electronic state of the defect. However, we show in what follows that this is not exact, and that the old expression for the line-shape function remains valid also for very narrow bands. As well as in Bohr's early theory for the hydrogen atom, a semiclassical reasoning leads to the right, fully quantal, result for this case.

To remark this, we review the general theory for the line shapes and then particularize to a situation in which the band width is smaller than the Debye energy of the solid. The resulting expression is used to analyze the experimental data on infrared absorption by the local modes of *U* centers in KCl and KBr, which show bands as narrow as 0.002–0.005 eV full width at half height.[6] *U* centers are substitutional H^- impurities. Though heavier and more localized than *F* centers, they are much lighter than the lattice normal constituents. To show the theory works well also for heavy de-

fects, we apply it also to reproduce the infrared absorption line shapes by Ag^+ impurities in KI. To our knowledge, no similar attempt has been published yet.

Infrared absorption lines are attributed to the local vibrational modes of the defect. Though narrow when compared with absorption lines of higher energy, their widths for U centers and heavier impurities in alkali halides are about 10% the Debye energy. This means that these modes are not free, but couple significatively with the rest of the crystal modes of vibration. In our analysis, they are dealt with as impurity states. The agreement attained between theory and experiment is remarkable, which allows one to understand the origin of the asymmetries that characterize the infrared absorption bands of defect centers in crystalline solids.

II. THE HAMILTONIAN

A. The main terms of the Hamiltonian

The crystalline solid interacting with the electromagnetic field is governed by the Hamiltonian

$$H = H_0 + H_1 + H_2 + H_3, \tag{1}$$

where

$$H_0 = \sum_q \hbar\omega_q a_q^\dagger a_q + \sum_l \epsilon_l c_l^\dagger c_l + \sum_{ql} g_{ql} c_l^\dagger c_l (a_q - a_{\bar{q}}^\dagger) \tag{2}$$

represents a crystal, eventually having point imperfections, whose atomic constituents can be in different internal states. The index $q=(\mu,\vec{q})$ denotes the vibrational mode of the branch μ whose wave vector, frequency, and polarization vector are $\vec{q}$, ω_q, and $\hat{e}_q$. The corresponding phonon operator is a_q. The branch index μ also characterizes localized modes associated to eventual crystal defects. We also denote $\bar{q} \equiv (\mu,-\vec{q})$. The fermion operator $c_l^\dagger$, where $l=(\alpha,\vec{l})$, creates an electron in state $\psi_\alpha(\vec{r}-\vec{l})$, bound to the ion at the lattice site $\vec{l}$, with α labeling the excitation state. The operator $c_l^\dagger c_l$ accounts for the internal state of the ion located at $\vec{l}$. By the hermiticity of H_0,

$$g_{ql}^* = -g_{\bar{q}l}. \tag{3}$$

The number operator $c_l^\dagger c_l$ has eigenvalues 0 and 1. The system represented by H_0 has a class of stationary states for which $\langle c_l^\dagger c_l\rangle = 0$ for any l, which is affected by just the first term of H_0. It describes the dynamics of the unperturbed harmonic crystal, in which all its ions are in their ground states. Then, the second and third terms of H_0 open chances for the internal states of the ions to be excited, or for the creation and annihilation of defects.

The electronic states α of the ionic core at $\vec{l}$ are described by the one-electron functions $\psi_\alpha(\vec{r}-\vec{l})$. For the F center, however, which is simply a single electron substituting a negative ion in an ionic crystal, or a neutral hydrogenic impurity, this conveys a mean field approximation for the electronic structure of the crystal ion at $\vec{l}$.

As the displacement of a lattice ion from its equilibrium position $\vec{l}$ is

$$\vec{u}_{\vec{l}} = \sum_q \hat{e}_q \sqrt{\frac{\hbar}{2NM_{\vec{l}}\omega_q}} e^{i\vec{q}\cdot\vec{l}} (a_q - a_{\bar{q}}^\dagger), \tag{4}$$

where $M_{\vec{l}}$ is the ionic mass and N the number of cells, the operators $a_q - a_{\bar{q}}^\dagger$ are essentially the Fourier components of the ionic motions around the lattice sites. Formally, the term H_0 is equivalent to the Hamiltonian of a set of uncoupled displaced harmonic oscillators, with the displacements proportional to the number operators $c_l^\dagger c_l$.

The next term of H

$$H_1 = \sum_{l\neq l'} \sum_q g_{ql'l} c_{l'}^\dagger c_l (a_q - a_{\bar{q}}^\dagger) \tag{5}$$

expresses that the internal dynamics of the crystal ions is disturbed by the presence of their neighbors. The diagonal electron-phonon coefficients g_{ql} are associated to local distortions of the lattice, whereas the terms in $g_{ql'l}$ may contribute to the hybridization of the electronic states, turning their energy levels into bands of finite width. Also, for l and l' such that $\vec{l}\neq\vec{l}'$, H_1 is a hopping term, describing electronic exchanges between the different ions. The sizes of the electron-phonon coefficients g_{ql} and $g_{ql'l}$ are expected to be very dissimilar, and H_1 is a comparatively small term. The neglection of H_1 is usually referred to as the Condon approximation. However, owing to the particularly strong electron-phonon couplings which characterize F centers, one may expect that, for these defects, H_1 will be large enough to produce observable effects.[5]

Alternatively, if one interprets that $c_l^\dagger$ and c_l create and annihilate an impurity in site $\vec{l}$, H_1 acquires a very interesting significance: a transition from $l=(\alpha,\vec{l})$ to $l'=(\alpha,\vec{l}')$ is a hopping of the defect between two lattice sites, with no change in its internal state α, and the transition probability per unit time of such processes is essentially the diffusion coefficient. Hence, in that case, H_1 governs the phonon-assisted quantum diffusion of the impurity.[7–11]

The remaining two terms of H

$$H_2 = \sum_{\nu\vec{k}} \hbar c k \eta_{\nu\vec{k}}^\dagger \eta_{\nu\vec{k}} \tag{6}$$

and

$$H_3 = \frac{e}{mc} \vec{A}(\vec{r}) \cdot \vec{p} \tag{7}$$

represent the Hamiltonian of the free electromagnetic field and its interaction with the electron, respectively. As usual, we adopt the Coulomb gauge and neglect the term quadratic in the vector potential $\vec{A}$, whose representation in a plane wave basis reads

$$\vec{A}(\vec{r}) = \sum_{\nu\vec{k}} \hat{e}_{\nu\vec{k}} \sqrt{\frac{2\pi\hbar c}{k}} \frac{1}{\sqrt{V}} e^{i\vec{k}\cdot\vec{r}} (\eta_{\nu\vec{k}} - \eta_{\nu(-\vec{k})}^\dagger), \tag{8}$$

where $\eta_{\nu\vec{k}}^\dagger$ creates a photon with well-defined momentum $\hbar\vec{k}$ and polarization index ν. The unit vector $\hat{e}_{\nu\vec{k}}$ determines the polarization direction of the field mode $(\nu\vec{k})$. Vector $\vec{p}$ in Eq. (7) denotes the momentum operator of the electron. When

expressed in terms of the electronic operators, H_3 takes the form

$$H_3 = \sqrt{\frac{c}{V}} \sum_{l'l} Q_{l'l\nu\vec{k}} c_{l'}^{\dagger} c_l (\eta_{\nu\vec{k}} - \eta_{\nu(-\vec{k})}^{\dagger}), \tag{9}$$

where $Q_{l'l\nu\vec{k}}$ is a coefficient.

The representation (8) of the electromagnetic field by plane waves is adequate to study the absorption of light quanta from a collimated beam. The boundary conditions for the spontaneous emission demand the use of the multipolar expansion of the field. Since both cases are formally similar, we consider in detail just the absorption processes.

B. The coefficients

The second quantized Hamiltonian (1) is related with its correspondent operator $\mathcal{H}$ in coordinate representation by

$$H = \int d^3\vec{r} \Psi^{\dagger}(\vec{r}) \mathcal{H}(\vec{r},\vec{p}) \Psi(\vec{r}), \tag{10}$$

where

$$\Psi(\vec{r}) = \sum_l c_l \psi_\alpha(\vec{r} - \vec{l}), \quad l = (\alpha, \vec{l}), \tag{11}$$

is the electron field operator. In terms of coordinate representation magnitudes, the coefficients appearing in the several terms of H are then

$$g_{ql} = \sqrt{\frac{\hbar}{2NM_{\vec{l}}\omega_q}} \hat{e}_q \cdot \sum_{\vec{l}'} e^{i\vec{q}\cdot\vec{l}'} \vec{F}_{\alpha(\vec{l}-\vec{l}')}, \tag{12}$$

where

$$\vec{F}_{\alpha(\vec{l}-\vec{l}')} = \int d^3\vec{r} \psi_\alpha^*(\vec{r}) \nabla v(\vec{r} - \vec{l}' + \vec{l}) \psi_\alpha(\vec{r}) \tag{13}$$

and $v(\vec{r}-\vec{l})$ is the screened potential energy of interaction between the electron and the nucleus at $\vec{l}$. The magnitude $\vec{F}_{\alpha(\vec{l}-\vec{l}')}$ is the unbalanced force between two ions at $\vec{l}$ and $\vec{l}'$, caused by the excitation of one of them.

Similarly, the off-diagonal coefficients $g_{ql'l}$ are

$$g_{ql'l} = \sqrt{\frac{\hbar}{2NM_{\vec{l}}\omega_q}} \hat{e}_q \cdot \sum_{\vec{l}''} e^{i\vec{q}\cdot\vec{l}''} \vec{F}_{\alpha'\alpha(\vec{l}'-\vec{l}'')(\vec{l}-\vec{l}'')}, \tag{14}$$

where

$$\vec{F}_{\alpha'\alpha(\vec{l}'-\vec{l}'')(\vec{l}-\vec{l}'')} = \int d^3\vec{r} \psi_{\alpha'}^*(\vec{r} - \vec{l}' + \vec{l}'') \nabla v(\vec{r}) \psi_\alpha(\vec{r} - \vec{l} + \vec{l}'') \tag{15}$$

and the coefficient appearing in H_3 is

$$Q_{l'l\nu\vec{k}} = \frac{e}{mc} \sqrt{\frac{2\pi\hbar}{k}} \hat{e}_{\nu\vec{k}} \cdot \vec{f}_{\vec{k}l'l}, \tag{16}$$

where e/m is the specific charge of the electron and

$$\vec{f}_{\vec{k}l'l} = -i\hbar \int d^3\vec{r} \psi_{\alpha'}^*(\vec{r} - \vec{l}') e^{i\vec{k}\cdot\vec{r}} \nabla \psi_\alpha(\vec{r} - \vec{l}). \tag{17}$$

III. THE STATIONARY STATES OF H_0

A. Energy spectrum and eigenvectors of H_0

The new Bose operators

$$b_q = a_q - \sum_l \frac{g_{\bar{q}l}}{\hbar\omega_q} c_l^{\dagger} c_l, \tag{18}$$

which satisfy the commutation relations

$$[b_q, c_l] = \frac{g_{\bar{q}l}}{\hbar\omega_q} c_l, \quad [b_q, c_l^{\dagger}] = -\frac{g_{\bar{q}l}}{\hbar\omega_q} c_l^{\dagger} \tag{19}$$

and

$$[b_q, c_l^{\dagger} c_l] = 0, \tag{20}$$

decouple H_0 and separate it into three commuting terms. In effect, using Eq. (18) to eliminate the operators a_q from the right-hand side of Eq. (2), H_0 becomes

$$H_0 = \sum_q \hbar\omega_q b_q^{\dagger} b_q + \sum_l \left(\epsilon_l - \sum_q \frac{|g_{ql}|^2}{\hbar\omega_q} \right) c_l^{\dagger} c_l + \sum_{l \neq l'} \frac{g_{ql} g_{\bar{q}l'}}{\hbar\omega_q} c_l^{\dagger} c_l c_{l'}^{\dagger} c_{l'}. \tag{21}$$

The first term represents the vibrational energy of the ions around their new equilibrium positions, the second one incorporates a lattice accommodation energy associated to each local electronic state, and the third is an interaction between different ions, mediated by the local distortions that their excited states produce in the lattice. Its general form is reminiscent of the interaction term of the Hubbard Hamiltonian,[14] and should determine lattice mediated correlations between point defects at high concentrations.

The eigenvalue spectrum of H_0 is made of direct sums of the eigenvalues of its three commuting terms. As we are interested in crystal states with just one excited ion, the third term of H_0 can be disregarded. The eigenenergies for a single excited ion are

$$E_{l\{n_q\}} = \sum_{\{n_q\}} \hbar\omega_q n_q + \epsilon_l - \sum_q \frac{|g_{ql}|^2}{\hbar\omega_q}, \quad n_q = 0,1,2,\ldots . \tag{22}$$

Using the commutation relations (19) and the property

$$[b_q, f(b_q^{\dagger})] = f'(b_q^{\dagger}), \tag{23}$$

where f is an analytic function and f' its derivative, valid for any set $\{b_q\}$ of Bose operators, it is readily shown that

$$b_q \exp\left(\sum_{lq} \frac{g_{\bar{q}l}}{\hbar\omega_q} c_l^{\dagger} c_l b_q^{\dagger} \right) \prod_l (c_l^{\dagger})^{\mu_l} |00\rangle = 0, \quad \mu_l = 0,1. \tag{24}$$

Here $|00\rangle$ denotes the ground state of the crystal, with no vibrational nor electronic excitations, which satisfies

$$a_q|00\rangle = 0. \tag{25}$$

Equation (24) defines the vibrational ground state of the crystal with a set of point defects in internal states α, located at those sites $\vec{l}$ for which $\mu_l = 1$.

In particular, for a single defect, the vibrational ground state is

$$|l0\rangle = \exp\left(\frac{1}{2}\sum_q \left|\frac{g_{\bar{q}l}}{\hbar\omega_q}\right|^2\right)\exp\left(\sum_q \frac{g_{\bar{q}l}}{\hbar\omega_q} b_q^\dagger\right)c_l^\dagger|00\rangle, \tag{26}$$

where the first exponential factor in the right hand side was introduced to ensure that $\langle 0l|0l\rangle = 1$. With this notation, Eq. (24) reduces to

$$b_q|l0\rangle = 0 \quad \text{for any } l. \tag{27}$$

The alternative expression for $|l0\rangle$

$$|l0\rangle = \exp\left[\sum_q \frac{g_{ql}}{\hbar\omega_q}(b_q + b_{\bar{q}}^\dagger)\right]c_l^\dagger|00\rangle \tag{28}$$

has the advantage of being expressed in terms of an unitary operator acting on the bare defect state $c_l^\dagger|00\rangle$. The state $|l0\rangle$ describes the point defect dressed by the virtual phonon cloud representing the distortion it produces in the host lattice. The equivalence between Eqs. (26) and (28) can be shown with the help of the identity $\exp(A+B)\exp([A,B]/2) = \exp A \exp B$, valid for any pair of operators A and B which commute with their commutator $[A,B]$.

Therefore, in general, the one-defect eigenvectors of H_0 are

$$|l\{n_q\}\rangle = \prod_q \frac{(b_q^\dagger)^{n_q}}{\sqrt{n_q!}}\exp\left[\sum_q \frac{g_{ql}}{\hbar\omega_q}(b_q + b_{\bar{q}}^\dagger)\right]c_l^\dagger|00\rangle. \tag{29}$$

As $\langle l0|l0\rangle = 1$, vectors (29) form an orthonormal set.

B. Some useful properties

The commutation relations (19) can be written as

$$c_l^\dagger b_q^\dagger = \left(b_q^\dagger - \frac{g_{ql}}{\hbar\omega_q}\right)c_l^\dagger, \quad c_l b_q^\dagger = \left(b_q^\dagger + \frac{g_{ql}}{\hbar\omega_q}\right)c_l, \tag{30}$$

and, applying these equations n times, one has that

$$c_l^\dagger (b_q^\dagger)^n = \left(b_q^\dagger - \frac{g_{ql}}{\hbar\omega_q}\right)^n c_l^\dagger, \quad c_l (b_q^\dagger)^n = \left(b_q^\dagger + \frac{g_{ql}}{\hbar\omega_q}\right)^n c_l, \tag{31}$$

which can be extended to any analytic function of $b_q^\dagger$. Recalling Eq. (28) and noticing that

$$[c_l, b_q + b_{\bar{q}}^\dagger] = [c_l^\dagger, b_q + b_{\bar{q}}^\dagger] = 0, \tag{32}$$

one can easily realize that

$$c_l^\dagger c_{l'}|l'0\rangle = \exp\left[\sum_q (G_{ql'} - G_{ql})(b_q + b_{\bar{q}}^\dagger)\right]|l0\rangle, \tag{33}$$

where we defined

$$G_{ql} \equiv \frac{g_{ql}}{\hbar\omega_q}. \tag{34}$$

Alternatively, in terms of just phonon creation operators,

$$c_l^\dagger c_{l'}|l'0\rangle = \prod_q \exp\left[-\frac{1}{2}|G_{ql'} - G_{ql}|^2 + (G_{\bar{q}l'} - G_{\bar{q}l})b_q^\dagger\right]|l0\rangle \tag{35}$$

and $c_l^\dagger c_{l'}|l''0\rangle = 0$ for any $l' \neq l''$.

Defining also

$$G_{ql'l} \equiv G_{ql'} - G_{ql}, \tag{36}$$

from relations (29), (31), and (35) one has that

$$\begin{aligned}\langle l\{n_q\}|c_l^\dagger c_{l'}|l'\{n_q + \mu_q\}\rangle &= \langle l0|\prod_q \exp\left(-\frac{1}{2}|G_{ql'l}|^2\right) \\ &\times \frac{b_q^{n_q}}{\sqrt{n_q!}}\frac{(b_q^\dagger + G_{ql'l})^{n_q+\mu_q}}{\sqrt{(n_q+\mu_q)!}}\exp(G_{\bar{q}l'}b_q^\dagger)|l0\rangle.\end{aligned} \tag{37}$$

Using the property $\langle l0|b_q^n f(b_q^\dagger)|l0\rangle = f^{(n)}(0)$, satisfied by any set of Bose operators and analytic function f, Eq. (37) can be written as

$$\begin{aligned}\langle l\{n_q\}|c_l^\dagger c_{l'}|l'\{n_q + \mu_q\}\rangle &= \prod_q \frac{\exp\left(-\frac{1}{2}|G_{ql'l}|^2\right)}{\sqrt{n_q!\,(n_q+\mu_q)!}} \\ &\times \frac{d^{n_q}}{dy^{n_q}}[(y + G_{ql'l})^{n_q+\mu_q}\exp(G_{\bar{q}l'l}y)]\Big|_{y=0}\end{aligned} \tag{38}$$

or, replacing $x = -G_{\bar{q}l'l}(y + G_{ql'l})$,

$$\begin{aligned}&\langle l\{n_q\}|c_l^\dagger c_{l'}|l'\{n_q + \mu_q\}\rangle \\ &= \prod_q \frac{\exp\left(\frac{1}{2}|G_{ql'l}|^2\right)}{\sqrt{n_q!\,(n_q+\mu_q)!}}\frac{1}{|G_{\bar{q}l'l}|^{\mu_q}}\frac{d^{n_q}}{dx^{n_q}}(x^{n_q+\mu_q}e^{-x})\Big|_{x=|G_{ql'l}|^2}.\end{aligned} \tag{39}$$

Recalling the Rodrigues formula $(d^n/dx^n)(x^{n+\mu}e^{-x}) = n!\,x^\mu e^{-x}L_n^\mu(x)$ for the generalized Laguerre polynomials $L_n^\mu(x)$ one finally obtains that

$$\begin{aligned}\langle l'\{n_q + \mu_q\}|c_{l'}^\dagger c_l|l\{n_q\}\rangle &= \prod_q \sqrt{\frac{n_q!}{(n_q+\mu_q)!}}\exp\left(-\frac{1}{2}|G_{ql'l}|^2\right) \\ &\times |G_{ql'l}|^{\mu_q}L_{n_q}^{\mu_q}(|G_{ql'l}|^2).\end{aligned} \tag{40}$$

The factor multiplying each Laguerre polynomial in the equation above is precisely its corresponding weight function.

IV. THE OPTICAL ABSORPTION AND EMISSION BANDS

A. Temperature-dependent transition rates

As long as the experimental setup selects only one-photon events, the observed transition rates between the states $|\phi\rangle$ of

the free electromagnetic field are of first order in the term H_3, which couples it with the charges. Thus, Fermi's golden rule is accurate enough to describe their energy transfers.

The matrix element of the interaction H_3 between the stationary states of H_0+H_2

$$\langle \phi' | \langle l' \{ n_q + \mu_q \} | H_3 | l \{ n_q \} \rangle | \phi \rangle \tag{41}$$

separates into two factors. The first one,

$$\sqrt{\frac{c}{V}} \sum_{\nu \vec{k}} Q_{l' l \nu \vec{k}} \langle \phi' | (\eta_{\nu \vec{k}} - \eta^{\dagger}_{\nu(-\vec{k})}) | \phi \rangle, \tag{42}$$

vanishes when $|\phi\rangle$ and $|\phi'\rangle$ does not differ in just a single photon. For annihilation of one photon $(\nu, \vec{k})$, $\langle \phi' | \eta_{\nu \vec{k}} | \phi \rangle = \sqrt{n_{\nu \vec{k}}}$, and $\langle \phi' | \eta^{\dagger}_{\nu \vec{k}} | \phi \rangle = 0$, with $n_{\nu \vec{k}}$ being the number of $(\nu, \vec{k})$ photons in the volume V. Other terms in the sum (42), with indices different from $(\nu, \vec{k})$, vanish as well. The second factor is the matrix element (40).

Therefore, denoting

$$J_{\nu \vec{k}} = \frac{n_{\nu \vec{k}}}{V} c \tag{43}$$

the density of flux of $(\nu, \vec{k})$ photons, the matrix element for absorption processes takes the general form

$$\begin{aligned} &\langle \phi' | \langle l' \{ n_q + \mu_q \} | H_3 | l \{ n_q \} \rangle | \phi \rangle \\ &= \sqrt{J_{\nu \vec{k}}} Q_{l' l \nu \vec{k}} \prod_q \sqrt{\frac{n_q!}{(n_q + \mu_q)!}} \\ &\times \exp\left(-\frac{1}{2} |G_{q l' l}|^2 \right) G^{\mu_q}_{q l' l} L^{(\mu_q)}_{n_q} (|G_{q l' l}|^2). \end{aligned} \tag{44}$$

The vibrational states of the crystal are not measured, hence the transition rates $w_{l' l \nu \vec{k}}$ must be summed over all possible quantum numbers of the crystal modes, weighing the initial ones with their thermodynamic probabilities. Therefore, for absorption

$$\begin{aligned} w_{l' l \nu \vec{k}} = \frac{2\pi}{\hbar} \sum_{\{n_q\}} \sum_{\{\mu_q\}} \frac{1}{Q_T} \exp\left(-\sum_q \frac{\hbar \omega_q}{k_B T} n_q \right) |\langle \phi' | \langle l' \{ n_q \\ + \mu_q \} | H_3 | l \{ n_q \} \rangle | \phi \rangle|^2 \delta\left(\sum_q \hbar \omega_q \mu_q + E'_l - E_l - \hbar c k \right), \end{aligned} \tag{45}$$

where Q_T is the partition function of the crystal modes, k_B the Boltzmann constant, and T the temperature. Replacing Eq. (44) and solving the sum over n_q with the help of the Hille-Hardy formula

$$\sum_{n=0}^{\infty} n! \frac{L^{(\mu)}_n(x) L^{(\mu)}_n(y)}{\Gamma(n+\mu+1)} z^n = \frac{(xyz)^{-\mu/2}}{1-z} \exp\left(-z \frac{x+y}{1-z} \right) I_{\mu}\left(2 \frac{\sqrt{xyz}}{1-z} \right), \tag{46}$$

where I_{μ} is the modified Bessel function of order μ, one obtains that

$$w_{l' l \nu \vec{k}} = \frac{2\pi}{\hbar} J_{\nu \vec{k}} |Q_{l' l \nu \vec{k}}|^2 F_{l' l}(\hbar c k; T), \tag{47}$$

where

$$\begin{aligned} F_{l' l}(\hbar c k; T) = \prod_q \exp\left[-|G_{q l' l}|^2 \coth\left(\frac{\hbar \omega_q}{2 k_B T} \right) \right] \\ \times \sum_{\mu_q = -\infty}^{\infty} e^{\hbar \omega_q \mu_q / 2 k_B T} I_{\mu_q}\left(\frac{|G_{q l' l}|^2}{\sinh\left(\frac{\hbar \omega_q}{2 k_B T} \right)} \right) \\ \times \delta\left(\sum_q \hbar \omega_q \mu_q + E_{l' l} - \hbar c k \right) \end{aligned} \tag{48}$$

and $E_{l' l} = E_{l'} - E_l$. Replacing the integral form for the δ function and then the generating function of the modified Bessel functions, one obtains the integral expression

$$\begin{aligned} F_{l' l}(\hbar c k; T) = \int_{-\infty}^{\infty} dt \exp\left\{ \sum_q |G_{q l' l}|^2 \right. \\ \times \left[-\coth\left(\frac{\hbar \omega_q}{2 k_B T} \right) (1 - \cos(\omega_q t)) \right. \\ \left. \left. + i \sin(\omega_q t) \right] \right\} \frac{\exp[i(E_{l' l}/\hbar - c k) t]}{2\pi\hbar} \end{aligned} \tag{49}$$

for the line-shape function, alternate to the phonon expansion (48).

B. The line-shape function

It is easy to show that

$$\int_{-\infty}^{\infty} d(\hbar c k) F_{l' l}(\hbar c k; T) = 1. \tag{50}$$

Hence, in the Condon approximation, the total rate of photon absorption events does not depend on temperature, its value is given by the factor multiplying $F_{l' l}(\hbar c k; T)$ in Eq. (47), and the line shape is entirely governed by the distribution (49).

Equation (49) has the form

$$F_{l' l}(\hbar c k; T) = \int_{-\infty}^{\infty} dt \Lambda_{l' l}(t, \hbar c k; T), \tag{51}$$

where

$$|\Lambda_{l' l}(t, \hbar c k; T)| = e^{-J_{l' l}(t;T)} \tag{52}$$

and

$$J_{l' l}(t; T) = \sum_q |G_{q l' l}|^2 \coth\left(\frac{\hbar \omega_q}{2 k_B T} \right) [1 - \cos(\omega_q t)]. \tag{53}$$

To gain insight on the general features of $F_{l' l}(\hbar c k; T)$, we derive here explicit expressions for the case of a substitutional point defect in a lattice having the KCl structure. In a first step, simple Debye and Einstein models are used to deal with the acoustic and optical modes of the crystal, and only nearest-neighbor interaction between the defect and the lat-

tice is assumed. It is easy to realize that the final conclusions, which are used later to justify a more general treatment, should remain valid also for the true vibrational modes and forces.

The mean force exerted by the defect over a neighboring ion can be written as $\vec{F}_{\vec{l}'}=F\hat{l}'$, where $\vec{l}'$ is the lattice vector connecting the two crystal sites, and then the coefficients (12) now read

$$g_{ql}=\sqrt{\frac{\hbar}{2NM\omega_q}}F\hat{e}_q\sum_{\vec{l}'}e^{i\vec{q}\cdot\vec{l}'}\hat{l}'. \tag{54}$$

In the KCl structure,

$$\vec{l}'=\frac{a}{2}(\pm\hat{\imath},\pm\hat{\jmath},\pm\hat{k}), \tag{55}$$

where a is the lattice parameter. Recalling that the polarization vectors $\hat{e}_{\mu\vec{q}}$, $\mu=1,2,3$, of the normal modes form an orthogonal basis for each $\vec{q}$, one can show that

$$\sum_{\mu}|G_{ql'l}|^2=\frac{2(\Delta F)^2}{NM\hbar\omega_q^3}\sum_{i=x,y,z}\sin^2\left(\frac{a}{2}q_i\right). \tag{56}$$

The constant $\Delta F=F'-F$ is the variation of the force exerted by the defect on its neighbors upon excitation.

Separating the sums over μ into acoustic and optical branches, the exponent $J_{l'l}(t;T)$ splits into two terms

$$J_{l'l}(t;T)=J_{l'l}^{(\mathrm{ac})}(t;T)+J_{l'l}^{(\mathrm{op})}(t;T). \tag{57}$$

In the Debye model for the acoustic modes

$$\omega_{\mu\vec{q}}=\begin{cases}v_s q, & q=|\vec{q}|\le q_D,\\ 0, & \text{otherwise},\end{cases} \tag{58}$$

where the speed of sound v_s does not depend on the branch index μ and $aq_D=2(3\pi^2)^{1/3}$ for the KCl structure. Substituting this and Eq. (56) in Eq. (53), and replacing

$$\sum_q\to\sum_\mu\frac{V}{(2\pi)^3}\int d^3\vec{q}, \tag{59}$$

one obtains the nonperiodic function of t

$$J_{l'l}^{(\mathrm{ac})}(t,T)=\frac{3(\Delta F)^2}{\pi^2\hbar\rho v_s^3}\int_0^{aq_D}\frac{dx}{x}\left(1-\frac{\sin x}{x}\right)\times\coth\left(\frac{\hbar v_s}{2ak_BT}x\right)\sin^2\left(\frac{v_s t x}{2a}\right), \tag{60}$$

where $\rho=NM/V$. More explicitly, in terms of the Debye temperature Θ_D,

$$J_{l'l}^{(\mathrm{ac})}(t,T)=\frac{3(\Delta F)^2}{\pi^2\hbar\rho v_s^3}\int_0^{6.187}\frac{dx}{x}\left(1-\frac{\sin x}{x}\right)\times\coth\left(8.081\times10^{-2}\frac{\Theta_D}{T}x\right)\times\sin^2(1.058\times10^{10}\Theta_D t x). \tag{61}$$

Assuming a fixed frecuency ω_0 for the optical modes, the same procedure gives the optical component

$$J_{l'l}^{(\mathrm{op})}(t,T)=\frac{3(\Delta F)^2}{\pi^2\hbar\rho v_s^3}\times1.422\coth\left(\frac{\hbar\omega_0}{2k_BT}\right)\sin^2\left(\frac{\omega_0 t}{2}\right), \tag{62}$$

which is periodic in t. In this way, $F_{l'l}(\hbar ck;T)$ is the Fourier transform of the product of a nonperiodic function with a periodic function of t.

On the other hand, for

$$F(\omega)=\int_{-\infty}^{\infty}dt f(t)g(t)e^{i\omega t}, \tag{63}$$

where $g(t+\tau)=g(t)$, one can write

$$F(\omega)=\sum_{n=-\infty}^{\infty}g_n\int_{-\infty}^{\infty}dt\ f(t)e^{i(\omega+2\pi n/\tau)t}, \tag{64}$$

where g_n is a Fourier coefficient. Then

$$F(\omega)=\sum_{n=-\infty}^{\infty}g_nF_1(\omega+2\pi n/\tau), \tag{65}$$

where

$$F_1(\omega)=\int_{-\infty}^{\infty}dt\ f(t)e^{i\omega t}. \tag{66}$$

Thus, if $F_1(\omega)$ is a sharp distribution whose width is much smaller than $2\pi/\tau$, the effect of the periodic function g is to produce a periodic series of copies of $F_1(\omega)$, modulated by the coefficients g_n. The shape of the peaks depends entirely on the nonperiodic function f.

In conclusion, for our purposes, we can attribute the line shape just to the acoustic modes of vibration, and the optical ones can be disregarded when shape is the only concern. However, the total area under the main peak ($n=0$) is influenced by the optical modes through the Fourier coefficient g_0 in Eq. (65). Although the total absorption is temperature independent, the area under just the main peak is reduced by the temperature-dependent coefficient g_0, which accounts for the area under the subsidiary maxima produced by the optical modes. Anyway, for the shape function of the main maximum (i.e., in the frequency range $|\omega|<\pi/\tau$), one can put

$$J_{l'l}(t;T)=J_{l'l}^{(\mathrm{ac})}(t;T). \tag{67}$$

An illustrative example is given by Fig. 1, which shows $J_{l'l}(t;T)$, as given by Eq. (61), for $\Theta_D=400$ K, $T=100$ K, and $3(\Delta F)^2/(\pi^2\hbar\rho v_s^3)=1$. The function does not diverge for $t\to\pm\infty$, but goes to a constant. Hence the integral $F_{l'l}(\hbar ck;T)$ has a component that diverges to a δ function centered at $\hbar ck=E_{l'l}$. This is called the zero-phonon line.

V. WIDE AND NARROW BANDS

A. The wide band approximation

The function $J_{l'l}(t;T)$ has a minimum and vanishes at $t=0$. The coefficients $G_{ql'l}$, and hence $J_{l'l}(t;T)$, are proportional to the variation ΔF_i of the forces exerted by the defect on the neighboring crystal ions. Index i denotes the order of

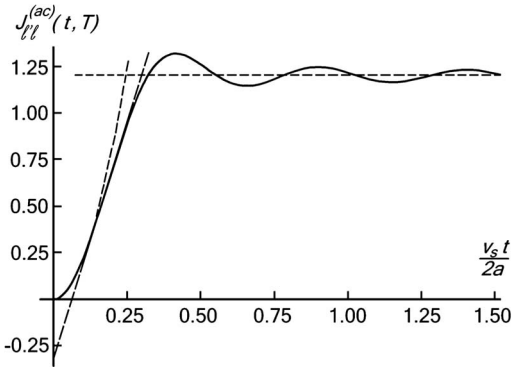

FIG. 1. The function $J_{l'l}^{(\mathrm{ac})}(t;T)$, as given by Eq. (61), for $T=100$ K and $\Theta_D=400$ K. Segmented lines represent the parabolic approximation (wide bands), the linear approximation (narrow bands), and the asymptotic behavior giving rise to the zero phonon line.

vicinity. If just one of these force variations is such that

$$\Delta F_i \gg \sqrt{\frac{\pi^2}{3}\hbar\rho v_s^3} \tag{68}$$

then $J_{l'l}(t;T)$ grows rapidly as t departs from $t=0$, $|\Lambda_{l'l}(t,\hbar ck;T)|$ falls rapidly to a very small constant, and the zero-phonon line is negligibly weak. For ΔF_i large enough, the absolute value of the subintegral function in Eq. (49) is significant only for $|\omega_D t| \ll \pi/2$. Replacing in it $1-\cos(\omega_q t) \approx \omega_q^2 t^2/2$ and $\sin(\omega_q t) \approx \omega_q t$, and then integrating, one obtains the Gaussian distribution

$$F_{l'l}(\hbar ck;T) = \frac{1}{\sqrt{\pi}\sigma_{l'l}(T)}\exp\left[-\frac{(\hbar ck - E_{l'l} - \Delta_{l'l})^2}{\sigma_{l'l}^2(T)}\right], \tag{69}$$

where the Stokes shift $\Delta_{l'l}$ is given by

$$\Delta_{l'l} = \sum_q \hbar\omega_q |G_{ql'l}|^2, \tag{70}$$

and whose standard deviation is

$$\sigma_{l'l}(T) = \left[2\sum_q \hbar^2\omega_q^2 |G_{ql'l}|^2 \coth\left(\frac{\hbar\omega_q}{2k_BT}\right)\right]^{1/2}. \tag{71}$$

The condition for this approximation to hold is

$$\sigma_{l'l}(T) \gg \frac{2\hbar\omega_D}{\pi}, \tag{72}$$

which is well satisfied at any temperature by F centers in ionic salts. In effect, Eqs. (69)–(71) fit the data on these defects within the experimental uncertainties.[5]

Additionally, from Eqs. (70) and (71) one has the simple relation between the Stokes shift and standard deviation of the bands at high temperatures

$$[\sigma_{l'l}(T)]^2 = 4k_B\Delta_{l'l}T \quad (T \gg \Theta_D/2). \tag{73}$$

Since the two quantities can be easily obtained from the experimentally measured bands, Eq. (73) provides a parameter-free test of theory. The data on F centers prove to follow quite accurately the asymptotic relation (73).[5]

B. Narrow bands

Equation (49) can be rewritten as

$$F_{l'l}(\hbar ck;T) = \int_{-\infty}^{\infty} dt \exp\left\{\sum_q |G_{ql'l}|^2\left[-2\omega_q^2 \coth\left(\frac{\hbar\omega_q}{2k_BT}\right)\times\left(\frac{\sin(\omega_q t/2)}{\omega_q}\right)^2 + i\omega_q\frac{\sin(\omega_q t)}{\omega_q}\right]\right\} \times \frac{\exp[i(E_{l'l}/\hbar - ck)t]}{2\pi\hbar}. \tag{74}$$

For large enough t,

$$\frac{\sin(\omega_q t)}{\omega_q} \approx \pi\delta_1(\omega_q)\frac{t}{|t|} \to \begin{cases} \pi\delta(\omega_q) & (t\to\infty), \\ -\pi\delta(\omega_q) & (t\to-\infty), \end{cases} \tag{75}$$

$$\left[\frac{\sin(\omega_q t/2)}{\omega_q}\right]^2 \approx \frac{\pi}{2}\delta_1(\omega_q)|t| \to \frac{\pi}{2}\delta(\omega_q)|t| \quad (t\to\pm\infty),$$

where δ_1 is a finite distribution which approaches a δ function for large t. Replacing in Eq. (74) and integrating one obtains that

$$F_{l'l}(\hbar ck;T) = \cos\ \delta_{l'l}F_{l'l}^{(e)}(\hbar ck;T) + \sin\ \delta_{l'l}F_{l'l}^{(o)}(\hbar ck;T), \tag{76}$$

where the first component of $F_{l'l}(\hbar ck;T)$ is the even Lorentzian distribution

$$F_{l'l}^{(e)}(\hbar ck;T) = \frac{1}{\pi}\frac{\Gamma_{l'l}(T)}{(\hbar ck - E_{l'l})^2 + [\Gamma_{l'l}(T)]^2} \tag{77}$$

and the second one is the odd function of $\hbar ck - E_{l'l}$

$$F_{l'l}^{(o)}(\hbar ck;T) = \frac{1}{\pi}\frac{\hbar ck - E_{l'l}}{(\hbar ck - E_{l'l})^2 + [\Gamma_{l'l}(T)]^2}. \tag{78}$$

$F_{l'l}^{(o)}(\hbar ck;T)$ gives account for the asymmetry of the band, which implicitly conveys a Stokes shift. The half width at half height of the distribution is

$$\Gamma_{l'l}(T) = \pi\sum_q \hbar\omega_q^2 |G_{ql'l}|^2 \coth\left(\frac{\hbar\omega_q}{2k_BT}\right)\delta_1(\omega_q) \tag{79}$$

and the constant $\delta_{l'l}$ governing the asymmetry reads

$$\delta_{l'l} = \pi\sum_q \omega_q |G_{ql'l}|^2 \delta_1(\omega_q). \tag{80}$$

The functions of $\vec{q}$ multiplying $\delta_1(\omega_q)$ in Eqs. (79) and (80) go to zero at $\vec{q}=0$, as ω_q does, and hence $\delta_1(\omega_q)$ cannot be replaced by a true δ function. The real meaning of δ_1 is that the region of the minimum of $J_{l'l}(t;T)$, shown in Fig. 1, gives the main contribution to the integral $F_{l'l}(\hbar ck;T)$. The approximation implicit in Eqs. (76)–(80) is to replace the

true function $J_{l'l}(t;T)$ by $J_{l'l}(t;T)=A_{l'l}|t|$, with $A_{l'l}$ depending only on ω_q, as is represented in Fig. 1 by the segmented straight line. The zone close to the minimum at $t=0$ is then approximated by a linear function, instead of a parabolic one, as was done for wide bands in the previous subsection.

To have an estimation for the error involved in the just explained approximation, recall that $F_{l'l}(\hbar ck;T)$ is normalized [Eq. (50)]. The Lorentzian function $F^{(e)}_{l'l}(\hbar ck;T)$ also encloses the unit area, but the integral of the odd component $F^{(o)}_{l'l}(\hbar ck;T)$ vanishes. Hence the area under the approximate distribution given by Eq. (76) is cos $\delta_{l'l}$, instead of unity. The error of the approximation can be estimated as the lost area, and is then of the order of $\delta^2_{l'l}$. The weight sin $\delta_{l'l}$ of the odd component is then within the range in which the approximation is valid.

The dispersion relations ω_q can be calculated from the force constants of the solid, which are known from neutron scattering experiments with high accuracy and for many materials. But for the force variations ΔF_i, this is the only input required by Eq. (49) or (74) to yield the line shape $F_{l'l}(\hbar ck;T)$ after a numerical integration. However, the approximate methods introduced in this section produce closed-form equations that give better insight in the origin of the general features displayed by the spectra.

VI. COMPARISON WITH EXPERIMENTAL RESULTS

The local modes of U centers and heavier impurities in alkali halides provide a good example of narrow photon absorption bands, showing the asymmetries predicted by Eqs. (76)–(78). Kittel's solid state textbook exhibits a beautiful example of such kind of asymmetric bands to illustrate optical absorption by localized modes in solids.[12] The spectral lines of U center modes and massive point defects are not sharp, but show bands whose widths are about 10% the Debye energy, indicating a rather strong interaction with the other degrees of freedom.

A main part of the harmonic forces between the crystal ions comes from the adiabatic shifts played by their electronic energies when the relative positions change. By virtue of the adiabatic approximation, the electronic degrees of freedom disappear and become implicit in the dynamics of the ions. Now we leave aside the adiabatic scheme for the U center, and take the substitutional H^- ion simply as a proton and two electrons trapped inside an anionic vacancy. The same strategy is applied to other impurities. From this viewpoint, the localized modes are electronic states, which we assimilate to the quantum numbers l and l'.

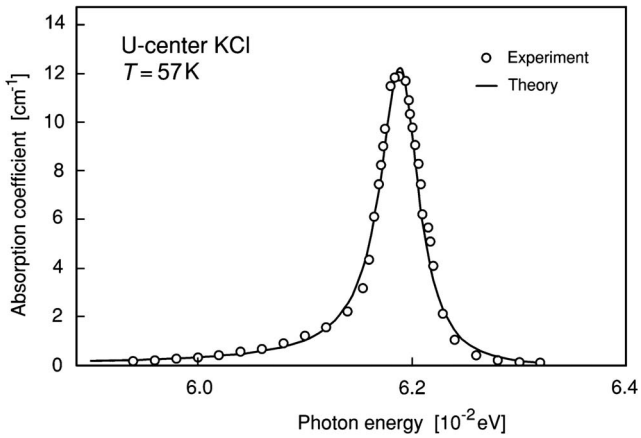

FIG. 2. Infrared absorption by localized modes of substitutional H^- (U center) in KCl at $T=57$ K. The circles represent experimental data of Schaefer (Ref. 6) and the solid line depicts Eqs. (76)–(78) with the parameters of Table I.

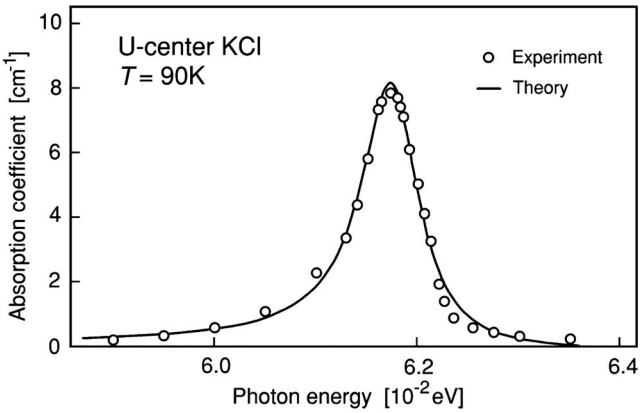

FIG. 3. Same as Fig. 2 but for $T=90$ K.

Figures 2 and 3 show part of the experimental data published by Schaefer[6] on the infrared absorption bands of U centers in KCl at $T=57$ and 90 K, together with the curves given by Eqs. (76)–(78). Experiment measures, for different photon energies $\hbar ck$, a magnitude that is essentially the transition rate $w_{l'l}(\hbar ck;T)$, which is, in turn, proportional to the normalized shape function $F_{l'l}(\hbar ck;T)$. Hence, there is a scale factor between the two magnitudes. To accomplish the comparison, we simply fitted the curve

$$F_{l'l}(\hbar ck;T)=\frac{A}{\pi}\frac{\Gamma\cos\delta+(\hbar ck-E_{l'l})\sin\delta}{(\hbar ck-E_{l'l})^2+\Gamma^2} \tag{81}$$

to each set of data, proceeding independently for $T=57$ and 90 K, choosing the parameters Γ and δ, which determine the shape, and the scale factor A. As discussed in Sec. IV, A is temperature dependent because of the coefficient g_0.

According to theory, δ should not depend on the temperature T. Table I shows the values of the parameters giving the curves of Figs. 2 and 3. As expected, the asymmetry parameter δ shows a small variation, but still within reasonable bounds. Since the error of the approximation can be estimated as δ^2, the uncertainty in $F_{l'l}(\hbar ck;T)$ is close to 2.5%. As the asymmetry is not very pronounced, small errors in $F_{l'l}(\hbar ck;T)$ may induce larger relative variations in δ.

TABLE I. U centers in KCl. Values for the parameters appearing in Eq. (81).

T (K)	A (cm^{-1})	$-\delta$ (rad)	Γ (10^{-2} eV)	$E_{l'l}$ (10^{-2} eV)
57	0.848	0.12	0.022	6.190
90	0.880	0.14	0.034	6.174

TABLE II. U centers in KBr. Values for the parameters appearing in Eq. (81).

T (K)	A (cm^{-1})	$-\delta$ (rad)	Γ (10^{-2} eV)	$E_{l'l}$ (10^{-2} eV)
57	2.138	0.077	0.0269	5.522
90	1.842	0.079	0.0572	5.505

A similar procedure was accomplished for the data on KBr,[6] and the results are displayed by Figs. 4 and 5 and Table II. The asymmetry parameter δ exhibits again small shift with temperature.

The parameter δ turns out to be negative in both cases. The next section is devoted to discuss the physical meaning of this circumstance.

At temperatures higher than 90 K the height of the spectral peaks fall rapidly [$\sim$2.5 cm^{-1} for both KCl and KBr at T=194 K (Ref. 6)], and the quality of the fit between the theoretical curves and the data become much worse. It is expected that the term H_1 of the Hamiltonian, which was neglected in the present analysis, would acquire increasing importance with temperature, because it is proportional to the vibrational amplitudes.

Experimental results published by Takeno and Sievers[15] provide a chance for testing the theory at lower temperatures and higher mass. Figures 6 and 7 show the fit of the theoretical expression (81) to part of the data of these authors for KI crystals with Ag^+ substitutional impurities. The fit of the theoretical curve to the experimental points is striking, and the parameters giving that fit, shown in Table III, exhibit the expected behavior: both δ and E have the same value at the two temperatures.

VII. THE SIGN OF $\delta_{l'l}$

By its definition (80), the constant $\delta_{l'l}$ is a positive magnitude. It determines both the asymmetry of the band and the Stokes shift. A positive value of $\delta_{l'l}$ modifies the maximum

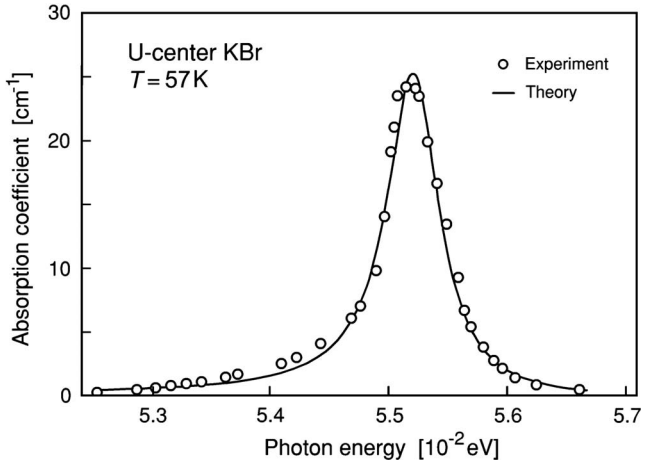

FIG. 4. Infrared absorption by U centers in KBr at T=57 K. The circles represent experimental data of Schaefer (Ref. 6) and the solid line depicts Eqs. (76)–(78) with the parameters of Table II.

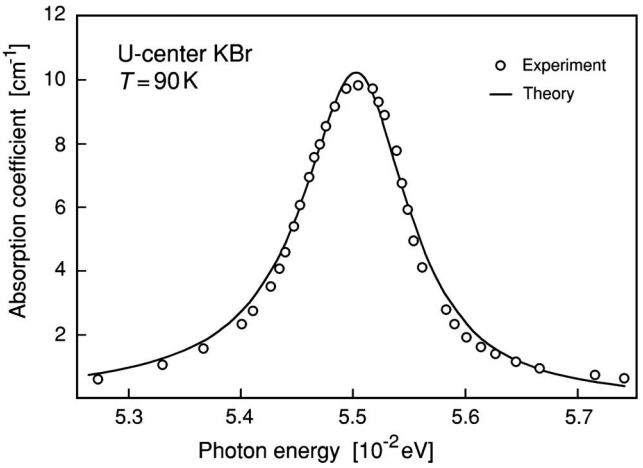

FIG. 5. Same as Fig. 4 but for T=90 K.

of the absorption band, and also the average photon energy transfer, to figures higher than $E_{l'l}$. This is the normal situation, because, in the mean, it is expected that the excitation processes be accompanied by phonon radiation seizing net energy. This can be seen also in the phonon exchange series, Eq. (48), whose terms are weighted by an exponential function of μ_q. Creation processes ($\mu_q > 0$) are then much more likely than annihilation ones.

For deexcitation processes, Eq. (48) holds as well, but with $-|E_{l'l}|+\hbar ck$ placed instead of $E_{l'l}-\hbar ck$ in the argument of the δ function. Now the term $\Sigma_{\mu_q}\hbar\omega_q\mu_q$, which is most likely positive, subtracts energy to the photons, and

$$\langle \hbar ck \rangle < |E_{l'l}|. \tag{82}$$

In the scheme of the previous sections, $\delta_{\ell'\ell} < 0$ for deexcitation of the defect.

Therefore, the theory suggests that the infrared absorption bands observed by Schaefer in KCl and KBr correspond to deexcitation processes. From this viewpoint, the initial impurity state is a metastable excited state, close to the ground

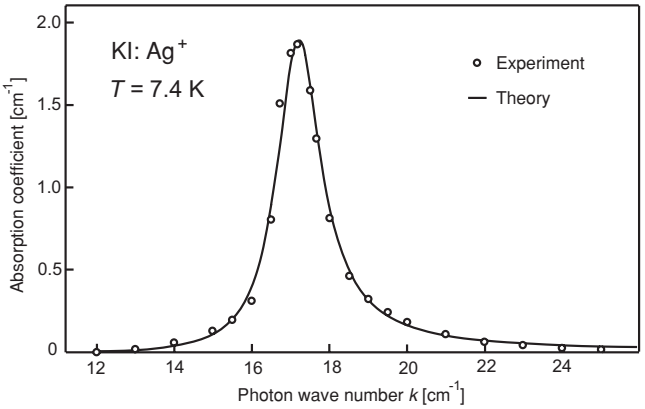

FIG. 6. Infrared absorption by Ag^+ in KI at T=7.4 K. The circles represent experimental data of Takeno and Sievers (Ref. 15), and the solid line depicts Eqs. (76)–(78) with the parameters of Table III.

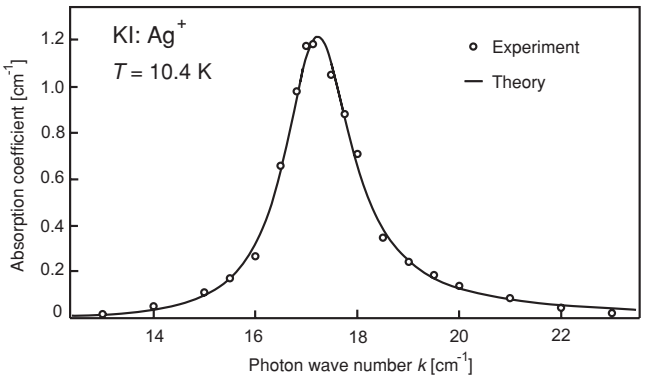

FIG. 7. Same as Fig. 6 but for $T=10.4$ K.

state, and the photon provides the energy necessary to jump over the potential barrier.

To understand the origin of this metastability, recall that we deal with states of very low energy, close to the Debye energy. On the other hand, the energy of a defect state l is of the general form

$$E_l = \epsilon_l - \sum_q \frac{|g_{ql}|^2}{\hbar\omega_q}, \tag{83}$$

where the term ϵ_l is the energy of the impurity in a rigid undeformed lattice, and the other term is the energy released by the lattice when reaching equilibrium with the impurity in state l. Calculations of the lattice relaxation energies show that they are of the order of the Debye energy,[13] and then the two terms of Eq. (83) are comparable. Hence, the different

TABLE III. Substitutional Ag in KI. Values for the parameters appearing in Eq. (81).

T (K)	A (cm^{-1})	δ (rad)	Γ (cm^{-1})	$E_{l'l}/\hbar c$ (cm^{-1})
7.4	4.21	0.12	0.70	17.17
10.4	3.08	0.12	0.80	17.17

eigenenergies E_l and their terms ϵ_l are not necessarily in the same order.

Consider two states l and l', such that

$$E_l > E_{l'}, \quad E_l < \epsilon_{l'}(l), \tag{84}$$

where $\epsilon_{l'}(l)$ is the energy of the defect state l', taking the lattice distortion caused by l as the reference undistorted lattice. According to the Franck-Condon principle, electronic excitations occur with no lattice modification, and lattice relaxation takes place subsequently. Therefore, the deexcitation process $l \to l'$ would follow the scheme

$$E_l \overset{(\hbar ck+\Delta)}{\longrightarrow} \epsilon_{l'}(l) \overset{(-\Delta')}{\longrightarrow} E_{l'}, \tag{85}$$

where Δ is an uncertainty in the energy transfer due to the fact that $\epsilon_{l'}(l)$ is not the energy of a true stationary state, and $\Delta-\Delta'$ is precisely the lattice relaxation energy.

ACKNOWLEDGMENTS

One author (M.L.) thanks the support by the Programa Bicentenario de Ciencia y Tecnología (Chile) ACT–26. F.A. is grateful to the Programa MECE Educación Superior for financial support.

*mlagos@utalca.cl

[1] K. Huang and A. Rhys, Proc. R. Soc. London, Ser. A **204**, 406 (1950).
[2] S. I. Pekar, Zh. Eksp. Teor. Fiz. **20**, 510 (1950).
[3] J. Franck, Trans. Faraday Soc. **21**, 536 (1926).
[4] E. U. Condon, Phys. Rev. **32**, 858 (1928).
[5] M. Lagos, R. Monreal, and J. Rogan, Phys. Status Solidi B **168**, 341 (1991).
[6] G. Schaefer, J. Phys. Chem. Solids **12**, 233 (1960).
[7] C. P. Flynn and A. M. Stoneham, Phys. Rev. B **1**, 3966 (1970).
[8] M. Lagos, Solid State Commun. **50**, 777 (1984).
[9] M. Lagos and H. Cerón, Solid State Commun. **65**, 535 (1988).
[10] M. Lagos, Solid State Commun. **69**, 11 (1989).
[11] M. Lagos and J. Rogan, Solid State Commun. **94**, 173 (1995).
[12] C. Kittel, *Introduction to Solid State Physics*, 4th ed. (John Wiley & Sons, New York, 1971).
[13] E. Miyoshi and S. Huzinaga, Phys. Rev. B **48**, 8583 (1993).
[14] J. Hubbard, Proc. R. Soc. London, Ser. A **276**, 238 (1963).
[15] S. Takeno and A. J. Sievers, Phys. Rev. Lett. **15**, 1020 (1965).